Cerebral Cortex, April 2017;27:2617–2627

doi:10.1093/cercor/bhw079
Advance Access Publication Date: 12 April 2016
Original Article

ORIGINAL ARTICLE

Functional Connectivity Between the Temporoparietal Cortex and Cerebellum in Autism Spectrum Disorder

Kajsa M. Igelström[1,2], Taylor W. Webb[1,2] and Michael S. A. Graziano[1,2]

[1]Princeton Neuroscience Institute and [2]Department of Psychology, Princeton University, Princeton, NJ 08544, USA

Address correspondence to Kajsa Igelström, Princeton Neuroscience Institute, Washington Road, Princeton, NJ 08544, USA. Email: kajsa@igelstrom.com

Abstract

The neural basis of autism spectrum disorder (ASD) is not yet understood. ASD is marked by social deficits and is strongly associated with cerebellar abnormalities. We studied the organization and cerebellar connectivity of the temporoparietal junction (TPJ), an area that plays a crucial role in social cognition. We applied localized independent component analysis to resting-state fMRI data from autistic and neurotypical adolescents to yield an unbiased parcellation of the bilateral TPJ into 11 independent components (ICs). A comparison between neurotypical and autistic adolescents showed that the organization of the TPJ was not significantly altered in ASD. Second, we used the time courses of the TPJ ICs as spatially unbiased "seeds" for a functional connectivity analysis applied to voxels within the cerebellum. We found that the cerebellum contained a fine-grained, lateralized map of the TPJ. The connectivity of the TPJ subdivisions with cerebellar zones showed one striking difference in ASD. The right dorsal TPJ showed markedly less connectivity with the left Crus II. Disturbed cerebellar input to this key region for cognition and multimodal integration may contribute to social deficits in ASD. The findings might also suggest that the right TPJ and/or left Crus II are potential targets for noninvasive brain stimulation therapies.

Key words: cerebellar Crus II, default mode network, developmental diaschisis hypothesis, frontoparietal executive resting-state network, localized independent component analysis

Introduction

Despite the ubiquity of brain imaging studies of autism spectrum disorder (ASD), there is little consensus on the neural basis of the disorder (Müller et al. 2011; Redcay et al. 2013; Tyszka et al. 2014). A prominent characteristic of ASD is significant deficits in social interaction and communication, functions that involve higher order regions of the cerebral cortex (Baron-Cohen et al. 1985; Castelli et al. 2002; Senju et al. 2009). Paradoxically, the brain structure that is most consistently abnormal in ASD is the cerebellum, which is best known for its role in motor coordination (Becker and Stoodley 2013; Wang et al. 2014). While the cerebellum is increasingly recognized to be involved in nonmotor functions (Strick et al. 2009), the role of the cerebellum in higher order behaviors is thought to be modulatory rather than causal (Schmahmann 2004). However, it has been proposed that loss of cerebellar function during sensitive periods of development may prevent normal maturation of nonmotor cortical neural circuitry (Wang et al. 2014). One possibility is, therefore, that ASD may involve disturbed connectivity between the cerebellum and areas of the cerebral cortex that mediate social cognition. The cerebellum is functionally connected to brain-wide cerebral resting-state networks, including higher order cognitive networks such as the frontoparietal control network (O'Reilly et al. 2010; Buckner et al. 2011). Several meta-studies mapping cerebellar activation clusters across different cognitive domains reported involvement in a large range of tasks involving mentalizing, working memory, executive function, and other behaviors (Stoodley and Schmahmann 2010; Keren-Happuch et al. 2014; Van Overwalle et al. 2014).

Recently our lab has focused on the functional organization of one part of the cerebral cortex that may mediate social cognition: the temporoparietal junction (TPJ) (Kelly et al. 2014; Igelström et al. 2015). The TPJ may be altered in autistic subjects. Adults

with high-functioning ASD were found to have altered white matter integrity of the TPJ (Barnea-Goraly et al. 2004; Mueller et al. 2013) and reduced functional connectivity within the default mode and theory-of-mind networks (Mueller et al. 2013; Kana et al. 2014). Reduced functional and structural connectivity in ASD has also been reported between the TPJ and the extrastriate cortex (Castelli et al. 2002; Barnea-Goraly et al. 2004). However, other studies examining functional connectivity in ASD have reported a lack of differences between neurotypical and autistic subjects (Müller et al. 2011; Redcay et al. 2013; Tyszka et al. 2014). These discrepancies may be related to the heterogeneous nature of ASD as well as methodological factors such as movement confounds (Müller et al. 2011; Redcay et al. 2013; Tyszka et al. 2014). The potential role of the TPJ and its connectivity in ASD pathophysiology is thus not yet understood. Posterior and anterior subregions of the right TPJ are functionally connected with different zones in the cerebellum (Mars et al. 2012), suggesting that the TPJ may be involved in more than 1 cerebro-cerebellar loop. Both the TPJ and the cerebellum are involved in multiple social and cognitive functions that may be disturbed in ASD, including theory-of-mind, episodic memory, emotional processing, and empathy (Bowler et al. 2000; Decety and Lamm 2007; Cabeza et al. 2012). Understanding the organization of the TPJ and TPJ-cerebellum connectivity in ASD is therefore an important goal.

Here, we studied the organization and cerebellar connectivity of the TPJ in neurotypical and autistic adolescents. We asked whether ASD is associated with disturbed organization of the TPJ and with disturbed connectivity between the TPJ and the cerebellum. We used local independent component analysis on fMRI resting-state data (local-ICA), a recent method for obtaining a fine-grained parcellation of spatially defined localized brain regions (Dobromyslin et al. 2012; Sohn et al. 2012; Beissner et al. 2014; Igelström et al. 2015). In our previous study, this method provided a parcellation of the TPJ into 9 main independent components (ICs), 5 in the right hemisphere and 4 in the left (Igelström et al. 2015). Here, to improve the thoroughness of the study, we expanded the cortical mask around the TPJ to include the more posterior temporoparietal cortex, and as a result, the parcellation yielded 11 ICs. We asked whether these local networks of the TPJ differed between adolescents with and without ASD. We then used the time courses of the ICs to study the functional connectivity between the TPJ subdivisions and the cerebellum. We chose to focus on these 2 brain regions with specific relevance to ASD, to enable us to conduct a spatially fine-grained analysis without the loss of statistical power that would result from a whole-brain analysis.

Materials and Methods

Subjects and Data

We used resting-state fMRI data available from the Autism Brain Imaging Data Exchange (ABIDE), a grass-root initiative that collects resting-state fMRI data from subjects with ASD and matched controls. The data were downloaded on 21 March 2015 and comprised all subjects (neurotypical and ASD) that had been scanned with the "UM MR" scanner according to the COINS database; http://coins.mrn.org). Although the ABIDE database contains data from multiple sites, we limited our study to subjects scanned with the same scanner, to minimize scanner-related variability in the data. The subject cohorts were scanned at the University of Michigan (Monk et al. 2009; Weng et al. 2010; Wiggins et al. 2011, 2012; funded by the National Institutes of Health, Autism Speaks, and Michigan Institute for Clinical and Health Research) and initially included individuals across the whole autism spectrum, 8–28 years of age (Samples 1 and 2, ABIDE).

The UM dataset was selected based on 2 general criteria: 1) >20 useable ASD subjects, aged <18, with a DSM-IV diagnosis of autistic disorder according to information provided on the ABIDE website (http://fcon_1000.projects.nitrc.org/indi/abide/) and 2) enough fMRI coverage of the cerebellum to allow statistical analysis of connectivity in the posterior lobe of the cerebellum. Unfortunately, even though the UM dataset showed good coverage of the Crus I and II (the main expected zones of TPJ connectivity), lobules VII–IX were incompletely sampled in many subjects (Fig. 1). Thus, it is important to note that the current study may overlook aberrant functional connectivity between the TPJ and the inferior cerebellum.

According to the initial investigators, ASD was diagnosed based on the Autism Diagnostic Interview Revised (ADI-R) (Lord et al. 1994), the Autism Diagnostic Observation Schedule (Lord et al. 2000) and clinical consensus. All ASD subjects had fluent language (based on completion of a valid Module 3 or 4 of the Autism Diagnostic Observation Schedule) and verbal IQ ≥ 80. Neurotypical controls were excluded if they received a score of ≥10 on the Social Communication Questionnaire (Rutter et al. 2003) or a score of ≥6 on the Obsessive/Compulsive subscale of the Spence Children's Anxiety Scale (Spence 1997).

The majority of ASD fMRI studies have included patients across the whole spectrum of autism, including subjects with Pervasive Developmental Disorder Not Otherwise Specified (PDD-NOS), and subjects with Asperger's Syndrome according to DSM-IV. Clinically, this range corresponds to a heterogeneous patient group, potentially explaining some of the variability present in published fMRI studies. We attempted to avoid some of this variability by studying a more homogenous sample. While

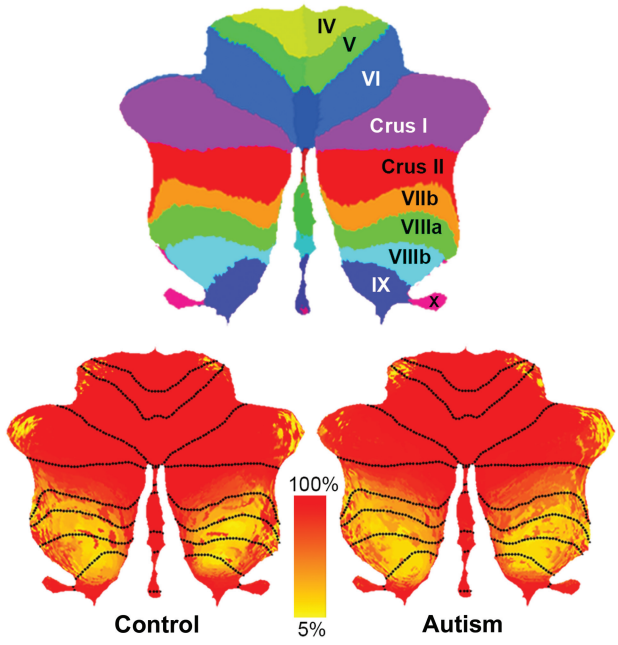

Figure 1. Coverage of the cerebellum in functional scans. The top image depicts the location of the cerebellar lobules on the flatmap according to the cerebellar SUIT atlas (Diedrichsen 2006; Diedrichsen et al. 2009; Diedrichsen and Zotow 2015). The lower panels are flatmaps showing cerebellar coverage (% of subjects) in the Control and ASD groups.

the use of ABIDE data precluded detailed clinical evaluation beyond what was reported by the original investigators, we applied exclusion criteria aimed to reduce the variability of the patient group. All decisions about the demographic balance were made before the data had been inspected or processed. From the original sample of 145 subjects (110 subjects in Sample 1; 35 subjects in Sample 2), we first excluded subjects with movement of >1 voxel in any direction (30 subjects: 8.5–17.4 years of age), followed by subjects above the age of 16 years (34 subjects: 17.1–28.8 years of age). The age range was chosen to compromise between maximizing age homogeneity and keeping enough subjects for meaningful analysis. Then, we excluded all subjects with a DSM-IV diagnosis of Asperger's syndrome, PDD-NOS or Unspecified (another 8 subjects: 10.4–16.1 years of age). Because the study could not be gender-balanced without excluding a prohibitively large number of subjects, females (13 subjects) were also excluded. The final dataset consisted of a sample of 60 male adolescents, aged 10.2–16.8. Twenty-six of the subjects had a DSM-IV diagnosis of ASD and 34 were neurotypical. There was no significant difference in age between the 2 groups (control 13.6 ± 0.37 years versus autism 13.8 ± 0.33 years; mean ± SE; $P = 0.70$, unpaired t-test). There was also no significant group difference in verbal IQ (control 113.7 ± 2.2 versus autism 111.0 ± 3.3; mean ± SE; $P = 0.48$) or performance IQ (control 104.4 ± 1.9 versus autism 105.4 ± 3.9; mean ± SE; $P = 0.80$). ADI-R scores of the ASD subjects were 20.4 ± 0.9 for social interactions, 15.9 ± 0.6 for language and communication, and 6.88 ± 0.5 for restrictive, repetitive, and stereotyped behaviors and interests.

The decision to exclude Asperger's syndrome was made based on the differences in clinical presentation required for a diagnosis according to the DSM-IV criteria (now outdated). By definition, the patients with Asperger's syndrome included in the original study must have shown normal development in areas outside social interaction, whereas patients diagnosed with ASD are likely to have shown more significant delays in communication. Thus, the exclusion of Asperger's syndrome is likely to have decreased the sample heterogeneity.

There was no significant difference in the maximum relative displacement between controls and autistic subjects (range 0.3–2.9 mm versus 0.4–2.8 mm, respectively; $P = 0.56$, unpaired t-test). Mean volume-to-volume 3D displacement (Van Dijk et al. 2012) did not differ significantly (control 0.049 ± 0.004 mm versus autism 0.057 ± 0.008 mm; mean ± SE; $P = 0.34$). The number of movements exceeding 0.1 mm between consecutive frames (Van Dijk et al. 2012) was not significantly different (median number of movements 18 in control versus 16.5 in autism; $P = 0.52$, Mann–Whitney U test).

MRI Data Acquisition

Data acquisition parameters have been described by the original investigators (Monk et al. 2009; Weng et al. 2010; Wiggins et al. 2011, 2012). Briefly, the data were acquired on a 3 T GE Signa scanner, using a reverse spiral sequence (TR = 2 s; TE = 30 ms; flip angle = 90°; 64 × 64 matrix; 40 axial slices, 3 mm thick). Structural images were acquired with a high-resolution T_1 scan (TR = 8.9 s; TE = 1.8 ms; flip angle = 15°; 256 × 160 matrix; 110 slices, 1.4 mm thick). Resting-state scans were 10 min long and participants fixated on a plus sign projected on a stimulus screen.

Preprocessing of fMRI Data

Preprocessing was done with AFNI (Cox 1996) and FSL (Jenkinson et al. 2012). The functional data were slice time-corrected and motion-corrected with FSL (Jenkinson et al. 2002), and then detrended (linear and quadratic) with AFNI. Single-session ICA was applied to each subject's unsmoothed functional data, and ICs that represented noise were regressed out using the FSL tool *fsl_regfilt* (Beckmann and Smith 2004; Kelly et al. 2010). The following spatial or temporal features were considered to represent noise as previously described (Kelly et al. 2010): spatial association with white matter, ventricles, or background voxels; time courses consisting of large spikes on a flat baseline; high-frequency noise; and temporal saw-tooth patterns likely to reflect cardiac or respiratory artifact. Such ICA-based denoising is effective in removing aberrant connectivity measures resulting from subject motion (Power et al. 2012; Salimi-Khorshidi et al. 2014; Pruim et al. 2015). During denoising, the investigator was blind to the subjects' diagnoses.

The denoised data were entered into 2 separate processing pipelines, 1 for the cerebrum and 1 for the cerebellum, to allow for cerebellum-specific spatial warping (Diedrichsen 2006; Diedrichsen et al. 2009). The position of the cerebellum varies between individuals, so conventional whole-brain warping causes severe misalignment and therefore loss of spatial specificity and statistical power. The cerebellum was isolated from the rest of the brain and aligned to the Spatially Unbiased Infratentorial (SUIT) atlas using the SUIT toolbox for SPM (Diedrichsen 2006; Diedrichsen et al. 2009). The deformation maps resulting from the structural transformation were used to align cerebellar functional data to the SUIT atlas. As a final step, all functional data were blurred to a final smoothness of 5 mm FWHM (3dBlurToFWHM in AFNI). Cerebral anatomical and functional data were spatially normalized to FSL's MNI-152 template with AFNI.

Group-Level Independent Component Analysis

We applied ICA on the group level on the voxels within a region of interest (ROI) mask. We used a modified version of the TPJ mask used in our previous study (Igelström et al. 2015). This was defined as the supramarginal gyrus, angular gyrus, posterior superior temporal gyrus, and posterior superior temporal sulcus in the Harvard–Oxford probabilistic brain atlas. Voxels anterior to $y = 16$ mm and ventral to $z = 0$ mm were excluded. Here, we expanded the mask to include the entire angular gyrus as defined by the standard MNI-152 brain template. The mask is shown in Figure 2. The reason for expanding the mask compared with our previous study was to ensure inclusion of the entirety of ICs in the angular gyrus. The mask covers a larger area than the regions thought to be involved in social processing. This is an advantage, because it allows a parcellation of the whole temporoparietal region, providing the opportunity to test the specificity of deficits and functions. It also provides a complete view of the mapping of the temporoparietal cortex in the cerebellum, which

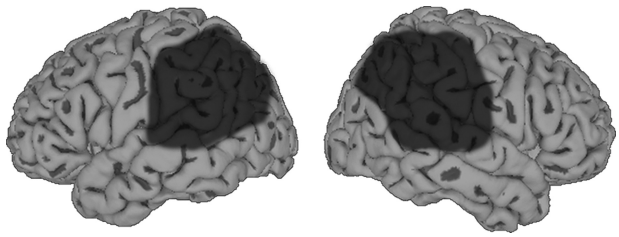

Figure 2. Mask used for group-level local-ICA. The region of interest included the supramarginal gyrus, angular gyrus, and the posterior superior temporal gyrus/sulcus.

has not previously been reported in detail. The reason for using localized ICA is that it allows a finer parcellation of the region (Sohn et al. 2012; Beissner et al. 2014; Igelström et al. 2015), but the exact extent of the mask is not critical for the results.

Probabilistic ICA was applied locally within the ROI (Fig. 2) on temporally concatenated resting-state data from all subjects (MELODIC toolbox in FSL; Beckmann and Smith 2004). We have previously shown that local-ICA identifies 4 TPJ subdivisions on the left side and 5 on the right (Igelström et al. 2015). The size and statistical properties of the ICs stabilized above ICA model orders of 20–30 and remained stable up to the highest model order tested ($d = 50$). In this study, we therefore used a high model order of $d = 50$ to maximize spatial specificity and separate all subdivisions into discrete right and left ICs.

To enable a voxel-wise statistical comparison of ICs between neurotypical and ASD subject, we used dual regression to derive subject-specific IC maps. This approach was developed by Beckmann and colleagues to estimate the spatial and temporal dynamics of ICs on the subject level, based on regression against the original fMRI data (Beckmann et al. 2009; Filippini et al. 2009). The dual regression consisted of 2 steps as described previously (Beckmann et al. 2009; Filippini et al. 2009). Briefly, the group-average set of spatial maps was first regressed (as spatial regressors in a multiple regression) into each subject's fMRI data, resulting in a set of subject-specific time series, one per group-level IC. Next, those time series were regressed (as temporal regressors) into the same fMRI data, resulting in a set of subject-specific spatial maps, one per group-level IC. Each IC was then compared between the neurotypical and autistic subjects using FSL's randomise permutation-testing tool (Winkler et al. 2014), and the P values were Bonferroni-corrected for the 11 comparisons.

Functional Connectivity Analysis

The CONN toolbox 15.c in SPM 12 (http://www.nitrc.org/projects/conn; Whitfield-Gabrieli and Nieto-Castanon 2012) was used for seed-to-voxel connectivity analysis (Biswal et al. 1995). Conventional bivariate correlation analysis was used, with the modification that the analysis was applied exclusively within the cerebellum (excluding the brainstem), and IC time courses were used instead of time courses from seed coordinates. The cerebellar mask was created by manually deleting brainstem voxels from a mask made from the SUIT template. The approach allowed data-driven identification of TPJ seed regions combined with cerebellum-specific functional connectivity analysis. The reason for using the IC time courses instead of averaged BOLD signal from a seed is that a higher signal-to-noise ratio is attained by data-driven separation of signal and noise processes. An averaged BOLD time course includes a summation of different processes, whereas an IC time course represents a process that has been "unmixed" from the summed signal. Although it presents significant strengths, this approach is uncommon, because ICA should be applied on a region that is spatially nonoverlapping with the region used in functional connectivity analysis. Because signals attributed to white matter, cerebrospinal fluid and subject motion had been regressed out of the data in the denoising step, we did not include these as regressors in the functional connectivity analysis, and global signal regression was not used. Verbal IQ, performance IQ and subject age were included as covariates on the second level. The connectivity analysis included all subjects, and the contrasts Autism > Control and Control > Autism were tested, while controlling for confounding effects of age and IQ. The normal connectivity patterns reported in Figure 3 are derived from the connectivity results in the neurotypical group.

A voxel-wise threshold of $P < 0.001$ uncorrected and a cluster extent threshold of $P < 0.05$ FDR-corrected were used. Voxels were considered to belong to a cluster if faces or edges touched. Additional Bonferroni correction was applied to correct for the 11 comparisons on the seed level. A 2-sample unpaired t-test was used to test for differences between neurotypical and autistic subjects ($P < 0.001$; Bonferroni-corrected on the seed level). Functional connectivity results are displayed on cerebellar flatmaps of the cerebellar SUIT atlas (Diedrichsen 2006; Diedrichsen et al. 2009; Diedrichsen and Zotow 2015).

Results

Cerebellar Coverage of Functional Scans

The functional scans covered a comparable range of the cerebellum in control and ASD subjects (Fig. 1). The coverage was good in the anterior lobe of the cerebellum as well as in the hemispheres of lobule VIIa (Crus I and II), the vermis, and lobule X. The Crus I/II are the cerebellar regions that are expected to have the greatest connectivity with social and cognitive regions of the TPJ, and therefore, these are the areas of greatest interest for the present comparison (Buckner et al. 2011). Coverage was less complete in the inferior cerebellum in lobules VIIb, VIIIa, and VIIIb, as shown in detail in Figure 1. Zones in lobules VIIIa and VIIIb were covered in the least number of subjects. Based on previously reported cerebro-cerebellar connectivity patterns, these inferior cerebellar zones probably do not connect to the social and cognitive TPJ regions (Buckner et al. 2011). Although we show all the connectivity data below, it is important to keep in mind that it is possible that there is aberrant connectivity of those areas of the cerebellum that is missed here due to incomplete sampling.

The Functional Organization of the Temporoparietal Cortex in Autism

We first applied local-ICA within an ROI around the TPJ (gray areas in Fig. 2), to obtain a functional parcellation on the group level (pooled neurotypical and autistic subjects, $n = 60$) (see Materials and Methods; Beckmann and Smith 2004; Kiviniemi et al. 2009; Igelström et al. 2015). This procedure identified the same subdivisions as we had previously reported (Igelström et al. 2015). Specifically, the ICs included a dorsal subdivision in the anterior angular gyrus (TPJd, dark blue in Fig. 3A), an anterior subdivision in the anterior supramarginal gyrus (TPJa, green in Fig. 3A), a ventral subdivision in the posterior superior temporal gyrus (TPJv, light yellow in Fig. 3A), a posterior subdivision located at the intersection between the angular, supramarginal, and superior temporal gyri (TPJp, red in Fig. 3A), and a central subdivision that was strongly right-biased (TPJc, orange in Fig. 3A). TPJd, TPJp, TPJa, and TPJv presented as separate left and right ICs, whereas TPJc presented as 1 right-biased IC, consistent with our previous study. We additionally report 2 symmetrical ICs located in the posterior angular gyrus, 1 right-sided and 1 left-sided (AGp, light blue in Fig. 3A).

Next, we tested for a difference in these 11 components between neurotypical and autistic subjects, using a dual regression approach with permutation testing (Filippini et al. 2009; Winkler et al. 2014; see Materials and Methods). None of the TPJ subdivisions differed between patients and controls, indicating that the functional organization of the temporoparietal cortex is intact in autistic adolescents, at least as measured with the current method.

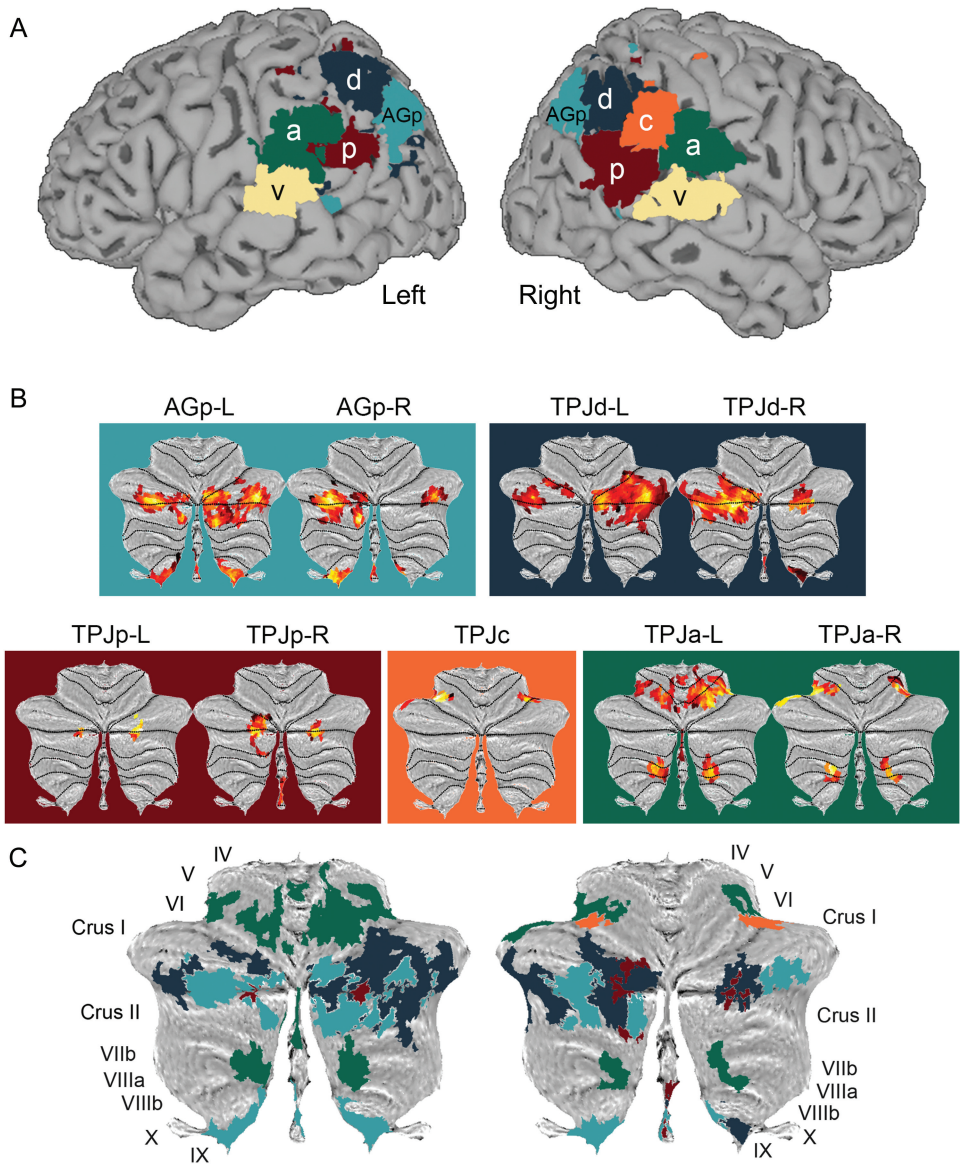

Figure 3. Connectivity between TPJ subdivisions and cerebellum. (*A*) Parcellation of the temporoparietal cortex with local independent component analysis (local-ICA; pooled control and autistic subjects, $n = 60$). Shown is a winner-take-all map of the 6 subdivisions in the right hemisphere and 5 subdivisions in the left hemisphere. Colors are matched across hemispheres for display purposes. Autistic subjects showed no difference in temporoparietal organization compared with neurotypical subjects (dual regression and permutation testing with FSL's randomise tool). (*B*) Normal functional connectivity of TPJ subdivisions with cerebellar zones. Shown are β coefficients projected onto cerebellar flatmaps. (*C*) Winner-take-all maps of β values for each TPJ subdivision, calculated separately for left and right TPJ (left and right panels, respectively). Colors are matched with A: TPJd, dark blue; AGp, light blue; TPJc, orange; TPJp, red; TPJa, green. TPJv (light yellow in A) showed no cerebellar connectivity.

Thus, despite the involvement of these cortical regions in social cognitive skills impaired in ASD, they showed no significant change in location, size, or conformation.

Cerebellar Maps of TPJ Subdivisions

We next tested whether the subdivisions of the TPJ described above were functionally connected to distinct cerebellar zones. The ICA technique identifies signal sources, each defined by a spatial probability distribution and a specific pattern of activity over time. Thus, each of the ICs is characterized by a time course. We used the time courses of the 11 ICs in the TPJ as seed time courses for functional connectivity analysis applied exclusively to the voxels within the cerebellum. A major advantage of using local-ICA to derive time courses is that it identifies TPJ "seed" time courses in a spatially unbiased way, avoiding the need for a subjective choice of seed coordinates in the TPJ (Beckmann and Smith 2004; Cole et al. 2010). As described in this section, the analysis revealed a fine-grained topographic map of the TPJ in the cerebellum (Fig. 3, Table 1).

The right and left TPJd (TPJd-R and TPJd-L) were functionally connected to the cerebellar hemispheres with a bias towards the contralateral side (dark blue in Fig. 3). The main clusters were located on the border between Crus I and Crus II. TPJp-R and TPJp-L were functionally connected to bilateral Crus I and II (red in Fig. 3), but to regions more medial than clusters corresponding to TPJd. TPJp-R and TPJp-L were also connected with contralateral lobule IX. TPJc was connected to bilateral regions

Table 1 Coordinates of cerebellar clusters functionally connected with TPJ subdivisions in the control group

TPJ subregion	Anatomical location of cluster peaks	MNI coordinates of peak β value (mm)			Cluster size (*N* voxels)	Cluster *P*-FDR
TPJd-R	Left Crus II	−30	−79	−38	347	<0.000001
	Right Crus II	+33	−79	−35	51	0.000005
	Right IX	+6	−55	−41	16	0.007025
TPJd-L	Right Crus II	+45	−67	−38	392	<0.000001
	Left Crus II	−45	−70	−38	48	0.000007
	Left Crus I	−30	−67	−29	21	0.001820
TPJp-R	Left Crus II	−21	−82	−35	69	0.000001
	Right Crus II	+24	−79	−35	17	0.011068
	Right IX	+3	−58	−38	13	0.003374
TPJp-L	Right Crus II	+24	−79	−35	25	0.001145
	Left Crus II	−24	−82	−35	10	0.037876
AGp-R	Left Crus II	−36	−73	−35	110	<0.000001
	Left IX	−9	−46	−41	67	<0.000001
	Left Crus II	−12	−85	−41	55	0.000002
	Right Crus II	+45	−64	−38	27	0.000374
AGp-L	Right Crus II	+45	−67	−38	244	<0.000001
	Right IX	+12	−52	−38	111	<0.000001
	Left Crus II	−36	−73	−38	78	<0.000001
	Left Crus II	−9	−85	−38	12	0.015049
	Left Crus II	−12	−82	−26	10	0.022808
TPJc	Right Crus I	+39	−55	−26	17	0.009997
	Left VI	−30	−52	−29	14	0.011564
TPJa-R	Left Crus II	−33	−46	−32	34	0.000413
	Right VI	+36	−46	−26	22	0.003088
	Right VIIIa	+18	−64	−50	16	0.009568
	Left VIIIa	−15	−64	−47	13	0.016616
TPJa-L	Right VI	+21	−58	−17	195	<0.000001
	Left dentate	−18	−61	−23	64	<0.000001
	Right VIIIa	+18	−67	−50	27	0.000426
	Left VIIIa	−15	−64	−44	22	0.001046
	Left VI	−30	−46	−29	14	0.006913

Shown are the anatomical labels (SUIT atlas), coordinates at the peak β value, cluster size, and *P* values of each statistically significant cluster (MNI-SUIT space).

between Crus I and lobule VI (orange in Fig. 3, right panel). TPJa-R and TPJa-L showed connectivity with lobules V and VI dorsally, and lobule VIII ventrally. This connectivity was bilateral but slightly biased towards the contralateral hemisphere (green in Fig. 3). TPJv showed no significant connectivity with the cerebellum. AGp-R and AGp-L were predominantly connected to Crus I and II dorsally and to the entire dorsoventral extent of lobule IX (light blue in Fig. 3). The connectivity of AGp was biased to the contralateral side.

In summary, the 3 most posterior TPJ subdivisions (TPJd, TPJp, and AGp) were connected to the cognitive regions of the cerebellum, TPJa was connected to motor regions, and TPJc was connected to a zone at the interface between cognitive and motor regions.

TPJ-Cerebellum Connectivity in Autism

Having established the fine-grained mapping of the TPJ onto the cerebellum, we asked whether the specific connectivity between the TPJ and the cerebellum showed any abnormalities in autistic subjects. The cerebellar connectivity with the TPJ subdivisions was compared between neurotypical and autistic subjects using second-level general linear model analysis with the between-subject contrasts Control > Autism and Autism > Control (CONN toolbox; Whitfield-Gabrieli and Nieto-Castanon 2012). Verbal and Performance IQ were included as covariates in the model. One subdivision, TPJd-R, showed significantly decreased connectivity with a region in left Crus II in autistic subjects compared with controls ($\beta = 0.16$, $t = 5.23$, $P < 0.001$; Bonferroni-corrected on the seed level and FDR-corrected on the cluster level; peak coordinates −27, −79, −38 mm, 25 voxels; Fig. 4).

One concern in this type of study is that there may be a gradation of subtle differences, only one of which happened to rise above the statistical threshold. In that case, the result would be dependent on the threshold, and it would be unjustified to point to a single component of the TPJ as the sole affected area. However, the present data do not follow that graded pattern. None of the other 10 subdivisions showed any alterations of cerebellar connectivity in ASD, even with relaxed statistical thresholds such as without correction for multiple comparisons. In contrast, the reduction in connectivity for the TPJd-R was highly significant after correction for multiple comparisons (seed level and cluster level, Materials and Methods).

Discussion

This study revealed a specific connectivity deficit between the right dorsal TPJ and left Crus II in ASD, despite apparently intact TPJ organization. We also found that local-ICA combined with functional connectivity analysis successfully resolved a fine-grained cerebellar map of the temporoparietal cortex.

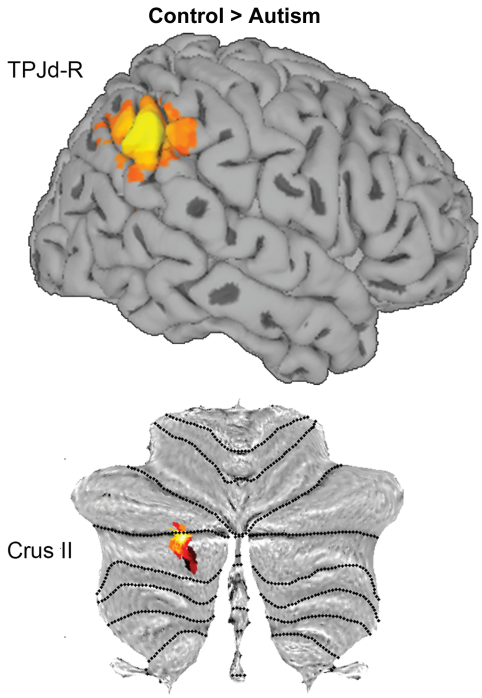

Figure 4. Decreased connectivity between TPJd-R and Crus II in ASD. The upper panel shows TPJd-R displayed on a right hemisphere surface (thresholded *Z* scores). The lower panel shows the region of significantly decreased functional connectivity in autistic subjects (β coefficients from 2-sample *t*-test, contrast Control > Autism.

Intact Functional Organization of the TPJ in ASD

We report that temporoparietal ICs are not significantly different between neurotypical and autistic adolescents. The finding suggests that local connectivity changes, which have been proposed to underlie ASD pathology (Belmonte et al. 2004; Rippon et al. 2007), may not be present within the temporoparietal cortex, since local connectivity is likely to influence the temporal correlations that define the ICs. Several previous studies have also failed to find connectivity abnormalities in ASD (Redcay et al. 2013; Tyszka et al. 2014). Taking together current and previous findings, it appears that abnormalities of the cerebral cortex in ASD are subtle and highly variable. Widespread nonfocal abnormalities seem to be a hallmark of the neurodevelopmental disorders, making it difficult to identify specific abnormalities that generalize to the whole patient population.

The apparent lack of autism-related changes in local TPJ networks is intriguing, but it is important to note that there are limitations that prevent strong conclusions. First, functional abnormalities may not be reflected by resting-state analysis unless accompanied by changes in topography, synchrony, or changes in low frequency power. More subtle differences may be apparent in task-based fMRI studies. For example, atypical BOLD responses have been reported in the right TPJ in mentalizing tasks in subjects with high-functioning ASD (Castelli et al. 2002; Lombardo et al. 2011). Second, even though our TPJ parcellation is fine-grained compared with descriptions of whole-brain resting-state networks, it is very likely that more fine-grained local networks exist. Thus, significant deficits may exist in more localized regions. Detection of such abnormalities is complicated by the great inter-subject variability in the temporoparietal cortex (Frederikse et al. 1999; Hasson et al. 2004; Van Essen 2005), so analysis on the individual subject level might be necessary.

Incomplete Coverage of the Cerebellum

A limitation of the current study is the incomplete coverage of voxels in lobules VIIb and VIII. However, these regions are mainly connected with networks outside the temporoparietal ROI (Buckner et al. 2011). They are activated by movement, working memory tasks, and verb generation, but not social cognition, story comprehension, or emotion (Stoodley et al. 2012; Diedrichsen and Zotow 2015). The left lobule VIIIb has been found to show gray matter reductions in ASD, but this region was associated with the somatomotor network (Stoodley 2014). Thus, while the regions of poor coverage in this study are of interest in ASD, they fall outside our focus on the TPJ and higher order functions. It is possible that the inferior parts of the cerebellum have aberrant connectivity with the TPJ in ASD that was not detected here due to under-sampling. Thus, the most cautious interpretation of the present study is that it provides a more detailed map of the known connections from the cerebellum to the TPJ in neurotypical subjects, and that it compares those connections to the same connections in subjects with ASD.

Topographic Map of the TPJ in the Cerebellum

Yeo et al. (2011) and Buckner et al. (2011) derived 7-network and 17-network parcellations of the cerebrum and cerebellum from resting-state data from 1000 subjects. Most resting-state networks were connected to zones in the cerebellum, and the posterior lobes of the cerebellum were connected with higher order areas. Our analysis, based on 60 subjects, resulted in cerebellar maps that were at least as fine-grained and additionally produced a split into left- and right-sided networks. Thus, our approach is a powerful method for studying TPJ-cerebellum connectivity. The cerebellum-specific spatial normalization combined with the use of IC time courses as "seeds" likely contributed to the ability to resolve these networks in a smaller cohort. Bernard et al. (2012) parcellated the cerebellum using a self-organizing map algorithm and found connectivity of clusters in Crus I and II with frontoparietal networks involving the inferior parietal lobule. Similar to the current study, their data-driven approach allowed unbiased identification of ROIs, although it still required averaging of BOLD time courses across voxels to derive seed time courses.

The connectivity findings provide some insights into the functions of the TPJ subdivisions reported here and in our previous study (Igelström et al. 2015). While the localization of the cerebellar connectivity of the posterior TPJ subdivisions was consistent with participation in higher order functions (Stoodley and Schmahmann 2010), the connectivity of TPJa suggests that it is less involved in the cognitive functions typically associated with the TPJ. This is also consistent with its anterior location, outside the region most often thought of as TPJ. The cerebellar connectivity of TPJc was markedly different from all the other subdivisions, with clusters on the border between the motor-related and cognitive lobes of the cerebellum. We previously showed that TPJc is part of the ventral attention network, and that TPJa is connected to similar networks but with more connectivity to motor-related regions (Igelström et al. 2015). Previous parcellation studies showed that TPJa/TPJc and their cerebellar clusters were merged into 1 network on the 7-network level and split into separate networks on the 17-network level (Buckner et al. 2011; Yeo et al. 2011). The cerebellar connectivity of the TPJc-containing network in the 17-network parcellation by Buckner et al. resembled the connectivity of TPJc, with clusters on the border between the cerebellar lobes. Taken together, the findings suggest that TPJc and TPJa are functionally related, and

that TPJc and its cerebellar counterpart are positioned at the interface between higher order regions and sensorimotor circuits. Deficits in functions associated with these regions of the TPJ are not typically associated with ASD, although there have been reports of abnormalities of bottom-up attention (Farrant and Uddin 2015; Keehn et al. 2016). The present results suggest that specific alterations of TPJ-cerebellum connectivity are not likely to underlie these deficits, but this must be tested specifically in task-based studies.

TPJp and AGp were both located in regions of the TPJ that have been associated with the default mode network (DMN), whereas TPJd was in a location consistent with participation in frontoparietal control networks (Buckner et al. 2008; Igelström et al. 2015). TPJp and AGp appeared as part of the DMN in the 7-network parcellation and as part of separate networks in the 17-network parcellation (Buckner et al. 2011; Yeo et al. 2011). Of the latter, 1 network included TPJp and showed strong involvement of frontal cortex and superior temporal sulcus. The other included AGp, medial prefrontal cortex, and precuneus (Yeo et al. 2011). The connectivity of the right TPJp with cerebellar Crus II is also consistent with a previous report of connectivity between a posterior subdivision of the right TPJ with left Crus II (MNI coordinates [−22, −84, −28] versus [−21, −82, −35] mm in the current study (Mars et al. 2012). The cerebellar connectivity patterns of AGp were similar to those of TPJp, but with a larger peak in the cerebellar tonsils and with Crus I/II peaks located lateral and medial to those of TPJp (Fig. 3). This observation may resolve some previous inconsistencies. While 1 study (Krienen and Buckner 2009) found that the DMN mainly connects with Crus I/II, another reported quite selective connectivity of the DMN with the cerebellar tonsils (Habas et al. 2009). This might be explained by that the latter study reported parietal DMN clusters in a location consistent with AGp (strongly connected to the cerebellar tonsils), whereas the former study used seed regions in medial prefrontal cortex and Crus I that are strongly connected with TPJp (Habas et al. 2009; Krienen and Buckner 2009). Both studies also used conventional alignment to an MNI template rather than cerebellum-specific warping, possibly preventing weakly connected clusters from being resolved (Diedrichsen 2006; Diedrichsen et al. 2009). The present results suggest that AGp and TPJp and their cerebellar counterparts represent 2 subcomponents of the DMN. The DMN is reciprocally regulated by the frontoparietal executive control network, which involves TPJd (Vincent et al. 2008; Chen et al. 2013). Both the DMN and frontoparietal control network have been associated with cognitive deficits in ASD (Just et al. 2007; Assaf et al. 2010). Multiple studies have reported abnormalities in the Crus I/II zones of connectivity with the posterior TPJ subdivisions in ASD (Becker and Stoodley 2013). Abnormalities in any network node within the frontoparietal or DMNs, including posterior TPJ subdivisions, cerebellar Crus I/II, or TPJ-Crus I/II connectivity, could potentially affect a wide range of functions, including core ASD symptoms such as social deficits.

TPJv, located around the auditory cortex, showed no connectivity with the cerebellum. This is consistent with previous studies in humans and rhesus monkeys, which showed a lack of connectivity between primary auditory cortex and cerebellum (Schmahmann and Pandya 1993; Krienen and Buckner 2009; Buckner et al. 2011).

TPJ-Cerebellum Connectivity in ASD

The decrease in connectivity in ASD was specific to TPJd-R/Crus II, arguing against the possibility that the finding reflected movement artifacts, which are suspected to be an uncontrolled confound in some studies showing long-range under-connectivity in ASD (Power et al. 2012; Satterthwaite et al. 2012; Van Dijk et al. 2012). If movement significantly influenced the apparent TPJ-cerebellum connectivity, this should have been seen for more than one of the TPJ subdivisions. Although movement artifacts can never be fully eliminated from studies with children and patient groups, we addressed these concerns by using a data-driven denoising technique and carefully balancing the control and ASD groups with respect to movement (Power et al. 2012; Salimi-Khorshidi et al. 2014; Pruim et al. 2015).

To our knowledge, this is the first study specifically examining connectivity between the cerebellum and subregions of the temporoparietal association cortex in ASD. The influence of the cerebellum on cerebral activity is not understood. Damage to the posterior lobe of the cerebellum can lead to cognitive and affective deficits, and it has been suggested that the cerebellum acts as an oscillation dampener that maintains cerebrocortical activity around a homeostatic baseline (Schmahmann and Sherman 1997; Schmahmann 2004). However, cognitive effects of cerebellar lesions are variable and difficult to interpret (Frank et al. 2007), highlighting the need for further studies. Wang et al. (2014) postulated that the cerebellum plays an important role in early development of cerebral function. When cerebellar deficits are inborn, cognitive impairments can be severe and may resemble ASD (Becker and Stoodley 2013). The cerebellum is often abnormal in ASD, and ASD susceptibility genes are strongly expressed in the cerebellum in the first years of life (Becker and Stoodley 2013; Menashe et al. 2013; Willsey et al. 2013; Wang et al. 2014). Volumetric studies on the cerebellum in ASD have revealed reductions in gray matter in several regions, with substantial variability across studies. In high-functioning adults, gray matter reductions were found in bilateral Crus I and in lobules VIII and IX (Rojas et al. 2006). In young children with low-functioning ASD, reduced gray matter volume in bilateral Crus II was correlated with social communication and interaction deficits (Riva et al. 2013). D'Mello et al. (2015) found reduced gray matter in right Crus I/II in autistic children that was correlated with the severity of social deficits and repetitive behaviors. Functional connectivity between the cerebellum and large cerebrocortical ROIs was decreased in supramodal regions such as the posterior parietal cortex (Khan et al. 2015). The roles of the cerebellum in the maturation of cerebral cortex and in cognitive function have yet to be elucidated, but our study suggests that ASD is associated with disturbance of normal communication between Crus II and TPJd-R. Here, we focused on a specific cortical ROI, to achieve high spatial specificity and limit the number of multiple comparisons. However, abnormalities in ASD may be widespread, and therefore, it will be important to also study the influence of the cerebellum on other cortical regions and wider brain networks.

TPJd is located in inferior parietal regions associated with semantic function and multimodal integration (Binder et al. 2009; Noonan et al. 2013). It also overlaps with loci of activation in theory-of-mind and attentional reorienting tasks (Dodell-Feder et al. 2011; Kubit and Jack 2013). This part of the cortex is highly lateralized, which may explain the unilateral nature of the connectivity deficit. For example, semantic function is dominant in the left angular gyrus, whereas attentional and social functions are thought to be right-lateralized (Saxe and Wexler 2005; Corbetta et al. 2008; Seghier 2013). ASD is associated with difficulties in integrating information, leading to a hyper-focus on details and an inability to see the big picture ("weak central coherence"; Happé and Frith 2006). Such detail-oriented processing may be related to deficits in high-level sensory integration and an increased

tendency to attend to behaviorally irrelevant targets (Marco et al. 2011). TPJd-R is thus positioned to be involved in the core deficits of ASD. TPJd-R is part of a right-lateralized frontoparietal network (Igelström et al. 2015) thought to be involved in executive control (Damoiseaux et al. 2006; Vincent et al. 2008). Autistic people have deficits in executive functions associated with under-connectivity between frontal and parietal regions (Ozonoff and Jensen 1999; Just et al. 2007). Reduced connectivity and atypical activation within default mode and frontoparietal networks have been reported to be associated with deficits in social interaction and communication (Assaf et al. 2010; O'Nions et al. 2014; Washington et al. 2014). It is therefore possible that disturbed cerebellar regulation of this key region of the right TPJ contributes to several important ASD symptoms.

These findings also suggest a possible new target for brain stimulation therapy. Studies have shown potential benefits of transcranial magnetic stimulation of the prefrontal cortex (Oberman et al. 2015). For example, bilateral stimulation of the dorsolateral prefrontal cortex, which is functionally connected to TPJd (Igelström et al. 2015), caused behavioral improvements and increased temporoparietal event-related potentials on EEG in autistic subjects (Sokhadze et al. 2014). Stimulation of Crus II and/or TPJd-R could in principle improve synaptic communication in this pathway and restore some function.

In summary, this study identified a novel connectivity deficit in young people with ASD. Despite apparently normal TPJ organization, there was a significant decrease in connectivity between the right TPJ and the left cerebellar Crus II. Understanding the influence of Crus II activity on right TPJ function during development may provide fundamental insights into ASD pathophysiology. In addition, the results suggest that Crus II and TPJd may be potential new targets for therapeutic intervention with brain stimulation.

Funding

This study was supported by the Princeton Neuroscience Institute Innovation Fund.

Notes

We thank Dr Joost Wiskerke for critical comments on the manuscript. *Conflict of Interest*: None declared.

References

Assaf M, Jagannathan K, Calhoun VD, Miller L, Stevens MC, Sahl R, O'Boyle JG, Schultz RT, Pearlson GD. 2010. Abnormal functional connectivity of default mode sub-networks in autism spectrum disorder patients. NeuroImage. 53:247–256.

Barnea-Goraly N, Kwon H, Menon V, Eliez S, Lotspeich L, Reiss AL. 2004. White matter structure in autism: preliminary evidence from diffusion tensor imaging. Biol Psychiatry. 55:323–326.

Baron-Cohen S, Leslie AM, Frith U. 1985. Does the autistic child have a "theory of mind"? Cognition. 21:37–46.

Becker EB, Stoodley CJ. 2013. Autism spectrum disorder and the cerebellum. Int Rev Neurobiol. 113:1–34.

Beckmann CF, Mackay CE, Fillippini N, Smith SM. 2009. Group comparison of resting-state fMRI data using multi-subject ICA and dual regression. NeuroImage. 47, Supplement 1:S148.

Beckmann CF, Smith SM. 2004. Probabilistic independent component analysis for functional magnetic resonance imaging. IEEE Trans Med Imaging. 23:137–152.

Beissner F, Schumann A, Brunn F, Eisenträger D, Bär K-J. 2014. Advances in functional magnetic resonance imaging of the human brainstem. NeuroImage. 86:91–98.

Belmonte MK, Allen G, Beckel-Mitchener A, Boulanger LM, Carper RA, Webb SJ. 2004. Autism and abnormal development of brain connectivity. J Neurosci. 24:9228–9231.

Bernard JA, Seidler RD, Hassevoort KM, Benson BL, Welsh RC, Wiggins JL, Jaeggi SM, Buschkuehl M, Monk CS, Jonides J, et al. 2012. Resting state cortico-cerebellar functional connectivity networks: A comparison of anatomical and self-organizing map approaches. Front Neuroanat. 6:31.

Binder JR, Desai RH, Graves WW, Conant LL. 2009. Where is the semantic system? A critical review and meta-analysis of 120 functional neuroimaging studies. Cereb Cortex. 19:2767–2796.

Biswal B, Yetkin FZ, Haughton V, Hyde J. 1995. Functional connectivity in the motor cortex of resting human brain using echo-planar MRI. Magn Reson Med. 34:537–541.

Bowler D, Gardiner J, Grice S. 2000. Episodic memory and remembering in adults with Asperger syndrome. J Autism Dev Disord. 30:295–304.

Buckner RL, Andrews-Hanna JR, Schacter DL. 2008. The brain's default network. Ann N Y Acad Sci. 1124:1–38.

Buckner RL, Krienen FM, Castellanos A, Diaz JC, Yeo BTT. 2011. The organization of the human cerebellum estimated by intrinsic functional connectivity. J Neurophysiol. 106:2322–2345.

Cabeza R, Ciaramelli E, Moscovitch M. 2012. Cognitive contributions of the ventral parietal cortex: an integrative theoretical account. Trends Cogn Sci. 16:338–352.

Castelli F, Frith C, Happé F, Frith U. 2002. Autism, Asperger syndrome and brain mechanisms for the attribution of mental states to animated shapes. Brain. 125:1839–1849.

Chen AC, Oathes DJ, Chang C, Bradley T, Zhou Z-W, Williams LM, Glover GH, Deisseroth K, Etkin A. 2013. Causal interactions between fronto-parietal central executive and default-mode networks in humans. Proc Natl Acad Sci USA. 110:19944–19949.

Cole DM, Smith SM, Beckmann CF. 2010. Advances and pitfalls in the analysis and interpretation of resting-state fMRI data. Front Syst Neurosci. 4:8.

Corbetta M, Patel G, Shulman GL. 2008. The reorienting system of the human brain: from environment to theory of mind. Neuron. 58:306–324.

Cox RW. 1996. AFNI: software for analysis and visualization of functional magnetic resonance neuroimages. Comput Biomed Res. 29:162–173.

Damoiseaux JS, Rombouts SARB, Barkhof F, Scheltens P, Stam CJ, Smith SM, Beckmann CF. 2006. Consistent resting-state networks across healthy subjects. Proc Natl Acad Sci USA. 103:13848–13853.

Decety J, Lamm C. 2007. The role of the right temporoparietal junction in social interaction: how low-level computational processes contribute to meta-cognition. Neuroscientist. 13:580–593.

Diedrichsen J. 2006. A spatially unbiased atlas template of the human cerebellum. NeuroImage. 33:127–138.

Diedrichsen J, Balsters JH, Flavell J, Cussans E, Ramnani N. 2009. A probabilistic MR atlas of the human cerebellum. NeuroImage. 46:39–46.

Diedrichsen J, Zotow E. 2015. Surface-based display of volume-averaged cerebellar imaging data. PLoS One. 10:e0133402.

D'Mello AM, Crocetti D, Mostofsky SH, Stoodley CJ. 2015. Cerebellar gray matter and lobular volumes correlate with core autism symptoms. NeuroImage Clinical. 7:631–639.

Dobromyslin VI, Salat DH, Fortier CB, Leritz EC, Beckmann CF, Milberg WP, McGlinchey RE. 2012. Distinct functional networks within the cerebellum and their relation to cortical systems assessed with independent component analysis. NeuroImage. 60:2073–2085.

Dodell-Feder D, Koster-Hale J, Bedny M, Saxe R. 2011. fMRI item analysis in a theory of mind task. NeuroImage. 55:705–712.

Farrant K, Uddin LQ. 2015. Atypical developmental of dorsal and ventral attention networks in autism. Dev Sci. doi:10.1111/desc.12359.

Filippini N, MacIntosh B, Hough M, Goodwin G, Frisoni G, Smith S, Matthews P, Beckmann C, Mackay C. 2009. Distinct patterns of brain activity in young carriers of the APOE-epsilon4 allele. Proc Natl Acad Sci USA. 106:7209–7214.

Frank B, Schoch B, Richter S, Frings M, Karnath H-O, Timmann D. 2007. Cerebellar lesion studies of cognitive function in children and adolescents—limitations and negative findings. Cerebellum. 6:242–253.

Frederikse ME, Lu A, Aylward E, Barta P, Pearlson G. 1999. Sex differences in the inferior parietal lobule. Cereb Cortex. 9:896–901.

Habas C, Kamdar N, Nguyen D, Prater K, Beckmann CF, Menon V, Greicius MD. 2009. Distinct cerebellar contributions to intrinsic connectivity networks. J Neurosci. 29:8586–8594.

Happé F, Frith U. 2006. The weak coherence account: detail-focused cognitive style in autism spectrum disorders. J Autism Dev Disord. 36:5–25.

Hasson U, Nir Y, Levy I, Fuhrmann G, Malach R. 2004. Intersubject synchronization of cortical activity during natural vision. Science. 303:1634–1640.

Igelström KM, Webb TW, Graziano MS. 2015. Neural processes in the human temporoparietal cortex separated by localized independent component analysis. J Neurosci. 35:9432–9445.

Jenkinson M, Bannister P, Brady M, Smith S. 2002. Improved optimization for the robust and accurate linear registration and motion correction of brain images. NeuroImage. 17:825–841.

Jenkinson M, Beckmann CF, Behrens TEJ, Woolrich MW, Smith SM. 2012. FSL. NeuroImage. 62:782–790.

Just MA, Cherkassky VL, Keller TA, Kana RK, Minshew NJ. 2007. Functional and anatomical cortical underconnectivity in autism: evidence from an fMRI study of an executive function task and corpus callosum morphometry. Cereb Cortex. 17:951–961.

Kana RK, Libero LE, Hu CP, Deshpande HD, Colburn JS. 2014. Functional brain networks and white matter underlying theory-of-mind in autism. Soc Cogn Affect Neurosci. 9:98–105.

Keehn B, Nair A, Lincoln AJ, Townsend J, Müller R-A. 2016. Underreactive but easily distracted: an fMRI investigation of attentional capture in autism spectrum disorder. Dev Cogn Neurosci. 17:46–56.

Kelly RE Jr, Alexopoulos GS, Wang Z, Gunning FM, Murphy CF, Morimoto SS, Kanellopoulos D, Jia Z, Lim KO, Hoptman MJ. 2010. Visual inspection of independent components: defining a procedure for artifact removal from fMRI data. J Neurosci Meth. 189:233–245.

Kelly YT, Webb TW, Meier JD, Arcaro MJ, Graziano MSA. 2014. Attributing awareness to oneself and to others. Proc Natl Acad Sci USA. 111:5012–5017.

Keren-Happuch E, Chen S-HA, Ho M-HR, Desmond JE. 2014. A meta-analysis of cerebellar contributions to higher cognition from PET and fMRI studies. Hum Brain Mapp. 35:593–615.

Khan AJ, Nair A, Keown CL, Datko MC, Lincoln AJ, Müller R-A. 2015. Cerebro-cerebellar resting-state functional connectivity in children and adolescents with autism spectrum disorder. Biol Psychiatry. 78:625–634.

Kiviniemi V, Starck T, Remes J, Long XY, Nikkinen J, Haapea M, Veijola J, Moilanen I, Isohanni M, Zang YF, et al. 2009. Functional segmentation of the brain cortex using high model order group PICA. Hum Brain Mapp. 30:3865–3886.

Krienen FM, Buckner RL. 2009. Segregated fronto-cerebellar circuits revealed by intrinsic functional connectivity. Cereb Cortex. 19:2485–2497.

Kubit B, Jack AI. 2013. Rethinking the role of the rTPJ in attention and social cognition in light of the opposing domains hypothesis: findings from an ALE-based meta-analysis and resting-state functional connectivity. Front Hum Neurosci. 7:323.

Lombardo MV, Chakrabarti B, Bullmore ET, Baron-Cohen S. 2011. Specialization of right temporo-parietal junction for mentalizing and its relation to social impairments in autism. NeuroImage. 56:1832–1838.

Lord C, Risi S, Lambrecht L, Cook E Jr, Leventhal B, DiLavore P, Pickles A, Rutter M. 2000. The Autism Diagnostic Observation Schedule—Generic: a standard measure of social and communication deficits associated with the spectrum of autism. J Autism Dev Disord. 30:205–223.

Lord C, Rutter M, Le Couteur A. 1994. Autism Diagnostic Interview-Revised: a revised version of a diagnostic interview for caregivers of individuals with possible pervasive developmental disorders. J Autism Dev Disord. 24:659–685.

Marco EJ, Hinkley LBN, Hill SS, Nagarajan SS. 2011. Sensory processing in autism: a review of neurophysiologic findings. Pediatr Res. 69:48R–54R.

Mars RB, Sallet J, Schüffelgen U, Jbabdi S, Toni I, Rushworth MFS. 2012. Connectivity-based subdivisions of the human right "temporoparietal junction area": evidence for different areas participating in different cortical networks. Cereb Cortex. 22:1894–1903.

Menashe I, Grange P, Larsen EC, Banerjee-Basu S, Mitra PP. 2013. Co-expression profiling of autism genes in the mouse brain. PLoS Comput Biol. 9:e1003128.

Monk CS, Peltier SJ, Wiggins JL, Weng S-J, Carrasco M, Risi S, Lord C. 2009. Abnormalities of intrinsic functional connectivity in autism spectrum disorders. NeuroImage. 47:764–772.

Mueller S, Keeser D, Samson AC, Kirsch V, Blautzik J, Grothe M, Erat O, Hegenloh M, Coates U, Reiser MF, et al. 2013. Convergent findings of altered functional and structural brain connectivity in individuals with high functioning autism: a multimodal MRI study. PLoS One. 8:e67329.

Müller R-A, Shih P, Keehn B, Deyoe JR, Leyden KM, Shukla DK. 2011. Underconnected, but how? A survey of functional connectivity MRI studies in autism spectrum disorders. Cereb Cortex. 21:2233–2243.

Noonan KA, Jefferies E, Visser M, Lambon Ralph MA. 2013. Going beyond inferior prefrontal involvement in semantic control: evidence for the additional contribution of dorsal angular gyrus and posterior middle temporal cortex. J Cogn Neurosci. 25:1824–1850.

Oberman LM, Enticott PG, Casanova M, Rotenberg A, Pascual-Leone A, McCracken J. 2015. Transcranial magnetic stimulation (TMS) therapy for autism: an international consensus conference held in conjunction with the international meeting for autism research on May 13th and 14th, 2014. Front Hum Neurosci. 8:1034.

O'Nions E, Sebastian CL, McCrory E, Chantiluke K, Happé F, Viding E. 2014. Neural bases of theory of mind in children with autism spectrum disorders and children with conduct problems and callous-unemotional traits. Dev Sci. 17:786–796.

O'Reilly JX, Beckmann CF, Tomassini V, Ramnani N, Johansen-Berg H. 2010. Distinct and overlapping functional zones in

the cerebellum defined by resting state functional connectivity. Cereb Cortex. 20:953–965.
Ozonoff S, Jensen J. 1999. Brief report: specific executive function profiles in three neurodevelopmental disorders. J Autism Dev Disord. 29:171–177.
Power JD, Barnes KA, Snyder AZ, Schlaggar BL, Petersen SE. 2012. Spurious but systematic correlations in functional connectivity MRI networks arise from subject motion. NeuroImage. 59:2142–2154.
Pruim RHR, Mennes M, Buitelaar JK, Beckmann CF. 2015. Evaluation of ICA-AROMA and alternative strategies for motion artifact removal in resting state fMRI. NeuroImage. 112:278–287.
Redcay E, Moran JM, Mavros PL, Tager-Flusberg H, Gabrieli JDE, Whitfield-Gabrieli S. 2013. Intrinsic functional network organization in high-functioning adolescents with autism spectrum disorder. Front Hum Neurosci. 7:573.
Rippon G, Brock J, Brown C, Boucher J. 2007. Disordered connectivity in the autistic brain: challenges for the 'new psychophysiology'. Int J Psychophysiol. 63:164–172.
Riva D, Annunziata S, Contarino V, Erbetta A, Aquino D, Bulgheroni S. 2013. Gray matter reduction in the vermis and Crus-II is associated with social and interaction deficits in low-functioning children with autistic spectrum disorders: a VBM-DARTEL study. Cerebellum. 12:676–685.
Rojas D, Peterson E, Winterrowd E, Reite M, Rogers S, Tregellas J. 2006. Regional gray matter volumetric changes in autism associated with social and repetitive behavior symptoms. BMC Psychiatry. 6:56.
Rutter M, Bailey A, Lord C. 2003. Social communication questionnaire (SCQ). Manual. Los Angeles: Western Psychological Services.
Salimi-Khorshidi G, Douaud G, Beckmann CF, Glasser MF, Griffanti L, Smith SM. 2014. Automatic denoising of functional MRI data: combining independent component analysis and hierarchical fusion of classifiers. NeuroImage. 90:449–468.
Satterthwaite TD, Wolf DH, Loughead J, Ruparel K, Elliott MA, Hakonarson H, Gur RC, Gur RE. 2012. Impact of in-scanner head motion on multiple measures of functional connectivity: relevance for studies of neurodevelopment in youth. NeuroImage. 60:623–632.
Saxe R, Wexler A. 2005. Making sense of another mind: the role of the right temporo-parietal junction. Neuropsychologia. 43:1391–1399.
Schmahmann JD. 2004. Cognition and the cerebellum. Neurology. 63:1991.
Schmahmann JD, Pandya DN. 1993. Prelunate, occipitotemporal, and parahippocampal projections to the basis pontis in rhesus monkey. J Comp Neurol. 337:94–112.
Schmahmann JD, Sherman JC. 1997. Cerebellar cognitive affective syndrome. Int Rev Neurobiol. 41:433–440.
Seghier ML. 2013. The angular gyrus: multiple functions and multiple subdivisions. Neuroscientist. 19:43–61.
Senju A, Southgate V, White S, Frith U. 2009. Mindblind eyes: an absence of spontaneous theory of mind in Asperger syndrome. Science. 325:883–885.
Sohn WS, Yoo K, Jeong Y. 2012. Independent component analysis of localized resting-state functional magnetic resonance imaging reveals specific motor subnetworks. Brain Connectivity. 2:218–224.
Sokhadze EM, El-Baz AS, Sears LL, Opris I, Casanova MF. 2014. rTMS neuromodulation improves electrocortical functional measures of information processing and behavioral responses in autism. Front Syst Neurosci. 8:134.
Spence SH. 1997. Structure of anxiety symptoms among children: a confirmatory factor-analytic study. J Abnorm Psychol. 106:280–297.
Stoodley CJ. 2014. Distinct regions of the cerebellum show gray matter decreases in autism, ADHD, and developmental dyslexia. Front Syst Neurosci. 8:92.
Stoodley CJ, Schmahmann JD. 2010. Evidence for topographic organization in the cerebellum of motor control versus cognitive and affective processing. Cortex. 46:831–844.
Stoodley CJ, Valera EM, Schmahmann JD. 2012. Functional topography of the cerebellum for motor and cognitive tasks: an fMRI study. NeuroImage. 59:1560–1570.
Strick P, Dum R, Fiez J. 2009. Cerebellum and nonmotor function. Annu Rev Neurosci. 32:413–434.
Tyszka JM, Kennedy DP, Paul LK, Adolphs R. 2014. Largely typical patterns of resting-state functional connectivity in high-functioning adults with autism. Cereb Cortex. 24:1894–1905.
Van Dijk KRA, Sabuncu MR, Buckner RL. 2012. The influence of head motion on intrinsic functional connectivity MRI. NeuroImage. 59:431–438.
Van Essen DC. 2005. A population-average, landmark- and surface-based (PALS) atlas of human cerebral cortex. NeuroImage. 28:635–662.
Van Overwalle F, Baetens K, Mariën P, Vandekerckhove M. 2014. Social cognition and the cerebellum: a meta-analysis of over 350 fMRI studies. NeuroImage. 86:554–572.
Vincent JL, Kahn I, Snyder AZ, Raichle ME, Buckner RL. 2008. Evidence for a frontoparietal control system revealed by intrinsic functional connectivity. J Neurophysiol. 100:3328–3342.
Wang SSH, Kloth AD, Badura A. 2014. The cerebellum, sensitive periods, and autism. Neuron. 83:518–532.
Washington SD, Gordon EM, Brar J, Warburton S, Sawyer AT, Wolfe A, Mease-Ference ER, Girton L, Hailu A, Mbwana J, et al. 2014. Dysmaturation of the default mode network in autism. Hum Brain Mapp. 35:1284–1296.
Weng S-J, Wiggins JL, Peltier SJ, Carrasco M, Risi S, Lord C, Monk CS. 2010. Alterations of resting state functional connectivity in the default network in adolescents with autism spectrum disorders. Brain Res. 1313:202–214.
Whitfield-Gabrieli S, Nieto-Castanon A. 2012. Conn: a functional connectivity toolbox for correlated and anticorrelated brain networks. Brain Connectivity. 2:125–141.
Wiggins JL, Bedoyan JK, Peltier SJ, Ashinoff S, Carrasco M, Weng S-J, Welsh RC, Martin DM, Monk CS. 2012. The impact of serotonin transporter (5-HTTLPR) genotype on the development of resting-state functional connectivity in children and adolescents: a preliminary report. NeuroImage. 59:2760–2770.
Wiggins JL, Peltier SJ, Ashinoff S, Weng S-J, Carrasco M, Welsh RC, Lord C, Monk CS. 2011. Using a self-organizing map algorithm to detect age-related changes in functional connectivity during rest in autism spectrum disorders. Brain Res. 1380:187–197.
Willsey AJ, Sanders Stephan J, Li M, Dong S, Tebbenkamp Andrew T, Muhle Rebecca A, Reilly Steven K, Lin L, Fertuzinhos S, Miller Jeremy A, et al. 2013. Coexpression networks implicate human midfetal deep cortical projection neurons in the pathogenesis of autism. Cell. 155:997–1007.
Winkler A, Ridgway G, Webster M, Smith S, Nichols T. 2014. Permutation inference for the general linear model. NeuroImage. 92:381–397.
Yeo BTT, Krienen FM, Sepulcre J, Sabuncu MR, Lashkari D, Hollinshead M, Roffman JL, Smoller JW, Zöllei L, Polimeni JR, et al. 2011. The organization of the human cerebral cortex estimated by intrinsic functional connectivity. J Neurophysiol. 106:1125–1165.